IEEE Access
Multidisciplinary | Rapid Review | Open Access Journal

Received November 18, 2018, accepted December 13, 2018, date of publication December 24, 2018,
date of current version January 11, 2019.

Digital Object Identifier 10.1109/ACCESS.2018.2889119

Artificial-Noise-Aided Precoding Design for Multi-User Visible Light Communication Channels

THANH V. PHAM[1], (Student Member, IEEE), TAKAFUMI HAYASHI[2], (Senior Member, IEEE), AND ANH T. PHAM[1], (Senior Member, IEEE)

[1]Computer Communications Laboratory, The University of Aizu, Aizuwakamatsu 965-8580, Japan
[2]Department of Information Engineering, Niigata University, Niigata 950-2181, Japan

Corresponding author: Thanh V. Pham (lete143@gmail.com)

This work was supported in part by the JSPS KAKENHI under Grant 18J14290 and Grant 15K00134.

ABSTRACT Recent developments in visible light communications (VLC) have focused on enhancing its security and privacy. This paper studies the physical layer security in VLC networks with multiple users when there is a single wiretap eavesdropper. In particular, our aim is to design the optimal artificial noise (AN)-aided precoding scheme to improve the secrecy performance in terms of legitimate users and eavesdropper's signal-to-interference-plus-noise ratios (SINRs). The purpose of our AN-aided precoding design is to ensure a fairness of the legitimate users' SINRs while impairing the quality of eavesdropper's channel as much as possible. Depending on the availability of the eavesdropper's channel state information (CSI) at the transmitters, there are generally two design strategies. When the eavesdropper's CSI is unknown to the transmitters (i.e., passive eavesdropper), the AN is constructed to be orthogonal to the users' aggregate channel matrix. In case the eavesdropper's CSI is available (i.e., active eavesdropper), the AN design strategy is to keep the SINR of the eavesdropper below a certain predefined threshold. Aside from the general design, we also study a specific design with the zero-forcing (ZF) technique and compare its performance with that of the general design. In both designs, numerical results show that significant gaps between users' and eavesdropper's SINR can always be achieved, thus guaranteeing a high secrecy performance. It is also observed that while the general design outperforms the ZF one in terms of the users' SINRs, it does not result in lower eavesdropper's SINRs compared to the ZF design, especially in the low transmit power region.

INDEX TERMS VLC wiretap channel, physical layer security, artificial noise-aided precoding, zero-forcing precoding.

I. INTRODUCTION

To address the tremendous demand for mobile data traffic given the spectrum scarcity problem in radio frequency (RF) communications, there has been a great deal of interest in research and development of optical wireless communications (OWC), which can be an alternative or complementary to the existing wireless technologies. In particular for indoor applications, visible light communications (VLC), which is a subset of OWC, has been gaining a lot of attention from both academia and industry thanks to the advances and massive deployment of light-emitting diodes (LEDs) over the last decade [1], [2].

Initially, research effort in VLC mainly focused on designing different methods to improve its performance and practicality [3]–[10]. Aside from these criteria, security and privacy are also important aspects in designing VLC systems. This is because the broadcast nature of visible light presents a challenge in guaranteeing secure and confidential communications in the presence of unauthorized users. Any users within the illuminated area can gain accessibility of the transmitted signals, thus making eavesdropping a possible threat. Traditionally, the security of data transmission is performed at network and transport layers by means of key-based cryptographic techniques. However, possible flaws in the mathematical foundation and recently discovered weaknesses of these techniques have motived researchers to look at another security measures [11]. In addition to security at upper layers, security at the physical layer (also known as physical layer security) has emerged as a completely new approach to deal with eavesdropping. The fundamental idea of physical layer security was initiated in the seminal work by Wyner [12], where he introduced the concept of wiretap

channel, which consists of a transmitter, a legitimate user and an eavesdropper. What makes physical layer security a promising alternative is that a perfect security can be achieved from information-theoretic information point of view. Additionally, the achieved security can also be precisely quantified by characterizing the *secrecy capacity*, which is defined as the transmission rate at which the eavesdroppers can not get any information from their eavesdropped messages regardless of their computational power and knowledge of the encoding scheme [13], [14]. Hence, it is widely believed that physical layer security is the strictest form of security.

In indoor environments, as a matter of fact that illumination is still the primary purpose, multiple LED arrays (LED luminaries) should be deployed to meet the lighting requirements. Naturally, this multi-LED transmitter configuration enables the multiple-input multiple-input (MIMO) transmission scheme. From the communications perspective, the benefit of the MIMO configuration is two-fold. Firstly, due to the low modulation bandwidth of the LEDs, achieving high data rate is one of the major concerns. The MIMO transmission can overcome the problem and provide high data rates by means of spatial multiplexing. Secondly, MIMO configurations can facilitate the achieving physical alignment between LED transmitters and mobile users. As a result, recent theoretical research and experiments on VLC have shifted to studying the potential of MIMO-VLC systems [8]–[10].

In the context of physical layer security, the inherent MIMO configuration introduces a spatial degrees of freedom, which can be utilized in the forms of precoding (i.e., beamforming) and/or artificial noise (AN) to enhance the secrecy capacity. Particularly, the use of precoding techniques for improving secrecy capacity was thoroughly studied in [15]–[17] for single-user and [18] for multi-user configurations under both perfect and uncertain channel state information (CSI) of the eavesdropper. The authors in [19] studied the secrecy outage probability (SOP) for a system consisting of multiple random distributed eavesdroppers. Based on the same performance metric (i.e., SOP), the work in [20] examined the use of non-orthogonal multiple access (NOMA) in multi-user multi-eavesdropper VLC systems. Most recently, the classical VLC wiretap channel (i.e., one transmitter, one legitimate user and one eavesdropper) has been revisited and analyses on lower and upper bounds of the secrecy capacity for this channel has been reported [21]. As for the AN approach, to the best of our knowledge, all previous studies focused on the single-user configuration only. In multi-transmitter configuration, there are generally two approaches of AN generation. On one hand, a set of LED transmitters is responsible for transmitting the AN to jam the eavesdropper's channel whereas the rest of the transmitters transmits the information-bearing signals to users [22], [23]. On the other hand, the AN could also be added to the precoded information-bearing signal as studied in recent works [24], [25]. The combined signal was then transmitted by all LED transmitters. This approach is known as AN-aided precoding and involves precoding designs for the AN and the information-bearing signals.

To the best of our knowledge, there is no study on AN-aided precoding design for physical layer security in multi-user VLC wiretap channels. We, therefore, attempts to fill this gap in this paper. As mentioned above, secrecy capacity is the main metric to evaluate the secrecy performance. Different from the complex and average power-constrained RF signal, the information signal in VLC is amplitude constrained [8]–[10]. This constraint makes the well-known Shannon capacity formula inapplicable for VLC channels. In fact, there is no closed-form expression for the capacity of an amplitude-constrained channel. Instead, it can be only be computed numerically through a complicated procedure [27]. The difficulty in characterizing the VLC channel capacity (and hence the secrecy capacity) lead to a challenge in designing AN-aided precoding with respective to the secrecy capacity. Therefore, we follow another approach for the AN design. Specifically, the AN design is based on the users's and the eavesdropper's signal-to-interference-plus-noise ratios (SINRs). In the conference version of the paper [26], we studied the design problems with respect to the max-min fairness of users's SINRs under the presence of an eavesdropper who can be either passive (i.e, its channel state information (CSI) is unknown by the transmitters) or active (i.e., its CSI is known by the transmitters). In the case of passive eavesdropper, the AN was designed to lie in the null space of users' aggregate channel matrix. We then investigated the impact of the AN noise power on the secrecy performances of users and the eavesdropper. In the case of active eavesdropper, the AN-aided precoding was designed taking into account a constraint that the eavesdropper's SINR is kept below a predefined threshold. In addition to the general design, in this paper, a specific design, which adopts the zero-forcing (ZF) technique as the underlaying precoding scheme for legitimate users, is also investigated. The purpose of ZF precoding is to decouple the multi-user channel to multiple subchanels, thus enabling confidentiality among legitimate users. A comprehensive comparison between the performances of general and ZF designs is then given.

The rest of the paper is structured as follows. In Section II, we explicitly describe the AN-aided precoding models for the considered multi-user VLC wiretap channel with respect to two different scenarios: passive and active eavesdropper. Section III focuses on the general AN-aided precoding designs while Section IV presents a specific design using ZF precoding scheme. Numerical results to compare the secrecy performances of the two design approaches are given in Section V. Section VI concludes the paper with some remarks.

Notation: The following notations are used throughout the paper. $\mathbb{R}$ and $\mathbb{E}[\cdot]$ are the set of real-valued numbers and the expected value operator, respectively. Bold upper case letters denotes matrices, e.g., $\mathbf{A}$ while the transpose of $\mathbf{A}$ is written as $\mathbf{A}^T$. $\|\cdot\|_1$ and $\|\cdot\|_F$ are the L_1 norm and the Frobenius norm, respectively. $\mathbf{I}_N$ denotes the identity matrix of size N, $\mathbf{e}_n$ is the all zero vector with the $n-$th element being 1, $\mathbf{1}_N$ is the

all one vector of size N, $\mathbf{0}_{M\times N}$ is all zero matrix of size $M\times N$. diag$\{\cdot\}$ and vec$(\cdot)$ indicate a square diagonal matrix and the vectorization operator. Finally, $\mathbf{A}\otimes\mathbf{B}$ and $\mathbf{A}\circ\mathbf{B}$ represent the Kronecker and the Hadamard products of matrices $\mathbf{A}$ and $\mathbf{B}$.

II. MULTI-USER WIRETAP VLC CHANNEL MODEL

A. VLC CHANNEL MODEL

As illustrated in Fig. 1, we consider in this paper a multi-user VLC wiretap channel, which consists of N_T LED arrays acting as the transmitters, K non-cooperative legitimate users and an eavesdropper. The K legitimate users are served by means of linear precoding techniques. Assume that users and the eavesdropper are each equipped with a photodiode (PD). For indoor scenarios, the light signal coming out from an LED transmitter reaches the receiver through multiple propagation paths due to refections off the surfaces. As a result, the channel response is the sum of the line-of-sight (LoS) component and multiple non light-of-sight (NLoS) ones. However, previous studies pointed that the LoS component is dominant over the NLoS ones as it accounts for more than 95% of the total received optical power at the receiver [28]. To simplify the analyses, we therefore consider the LoS propagation path only. Let $h_{n,k}$ be the LoS channel response coefficient between the $n-$th LED array and the $k-$th legitimate user, it is given by [28]

$$h_{n,k}=\begin{cases}\dfrac{A_r}{t_{n,k}^2}L(\phi)T_s(\psi_{n,k})g(\psi_{n,k})\cos(\psi_{n,k}), & 0\le\psi_{n,k}\le\Psi,\\ 0, & \psi_{n,k}>\Psi,\end{cases}\tag{1}$$

where A_r and $t_{n,k}$ are the active area of the PD and the link length, respectively. $L(\phi)$ is the emission intensity of a Lambertian light source

$$L(\phi)=\frac{l+1}{2\pi}\cos^l(\phi),\tag{2}$$

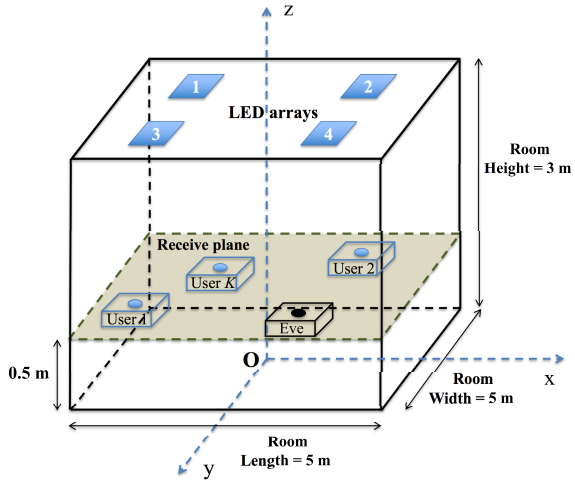

FIGURE 1. A geometrical configuration of multi-user VLC networks with an eavesdropper.

with ϕ being the angle of irradiance and l being the order of Lambertian emission determined by $l=-\frac{\log(2)}{\log(\Phi_{1/2})}$ where $\Phi_{1/2}$ is the LED's semi-angle for half illuminance. Ψ denotes the optical field of view (FOV) of the PD, $\psi_{n,k}$ is the angle of incidence and $T_s(\psi_{n,k})$ is the gain of the optical filter, whereas $g(\psi_{n,k})$ is the gain of the optical concentrator and is given by

$$g(\psi_{n,k})=\begin{cases}\dfrac{\kappa^2}{\sin^2\Psi}, & 0\le\psi_{n,k}\le\Psi,\\ 0, & \psi_{n,k}>\Psi,\end{cases}\tag{3}$$

where κ is the refractive index of the concentrator.

B. AN-AIDED PRECODING MODEL

Let $d_k\in\mathbb{R}$, which is drawn from the pulse amplitude modulation (PAM), be the data symbol for the $k-$th user. Additionally, let us denote $\mathbf{d}=\begin{bmatrix}d_1 & d_2 & \dots & d_K\end{bmatrix}^T\in\mathbb{R}^{K\times 1}$ be the users' data vector. Without loss of generality, suppose that d_k is zero mean and is uniformly distributed in the range of $[-1, 1]$. At the $n-$th LED array transmiter, the information-bearing signal s_n is generated from a linear combination of the data vector and a precoder $\mathbf{V}_n=\begin{bmatrix}w_{n,1} & w_{n,2} & \dots & w_{n,K}\end{bmatrix}\in\mathbb{R}^{1\times K}$ as

$$s_n=\mathbf{V}_n\mathbf{d}.\tag{4}$$

The basic idea of AN-aided precoding is to add a jamming signal (possibly after being precoded) to the information-bearing signal s_n. In the following, we explicitly describe the AN-aided precoding models for two scenarios: passive and active eavesdropper.

1) PASSIVE EAVESDROPPER

In the case of passive eavesdropper (i.e., the transmitters do not have any knowledge of the eavesdropper's CSI), a common strategy is to design the AN in such a way that it is orthogonal to the information-bearing signal. Hence, the AN does not impact the legitimate users' channels but could potentially impair the eavesdropper's channel quality. For this purpose, let $\mathbf{H}_k=\begin{bmatrix}h_{1,k} & h_{2,k} & \dots & h_{N_T,k}\end{bmatrix}\in\mathbb{R}^{1\times N_T}$ be the $k-$th user's channel matrix whose elements are given by (1). Also, let use define $\mathbf{H}=\begin{bmatrix}\mathbf{H}_1^T & \mathbf{H}_2^T & \dots & \mathbf{H}_K^T\end{bmatrix}^T\in\mathbb{R}^{K\times N_T}$ be the legitimate users' aggregate channel matrix. Assume that $\mathbf{H}$ is full row-rank and let $\mathbf{G}$, which is the precoder of the AN, be an orthonormal basis for the null-space of $\mathbf{H}$. According the rank-nullity theorem, rank$(\mathbf{H})$ + dim$(\mathbf{G})=N_T$. Since rank$(\mathbf{H})=K$, $\mathbf{G}$ has a dimension of (N_T-K). Hence, it can obviously be seen that this AN design is not feasible when $N_T\le K$. Throughout this paper, we thus assume that $N_T>K$. Denote $\mathbf{z}=\begin{bmatrix}z_1 & z_2 & \dots & z_{N_T-K}\end{bmatrix}^T\in\mathbb{R}^{(N_T-K)\times 1}$ as the AN noise vector, which is added into the information-bearing signal s_n. It is also assumed that each element z_i is zero mean and is uniformly distributed in the range of $[-1, 1]$. The broadcast signal at the $n-$th LED array can be written as

$$x_n=s_n+\rho_n\mathbf{G}_n\mathbf{z},\tag{5}$$

where $\mathbf{G}_n\in\mathbb{R}^{1\times(N_T-K)}$ is the $n-$th row vector of $\mathbf{G}$ and ρ_n is a constant, which controls the amplitude of the AN

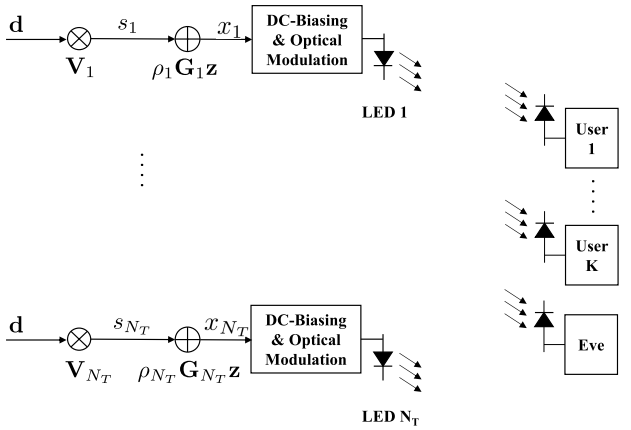

FIGURE 2. Schematic diagram of AN-aided precoding scheme: passive eavesdropper.

signal at the $n-$th LED transmitter (Fig. 2). Since d_i and z_i can take values between $[-1, 1]$, the broadcast signal x_n can take on negative values. However, VLC systems utilize intensity modulation/direction detection (IM/DD) scheme, which requires a non-negativity constraint on the LEDs' drive current. As a result, a DC-bias should be added into x_n to ensure that it is non-negative, that is

$$u_n = x_n + I_n^{\mathrm{DC}} \geq 0, \tag{6}$$

where I_n^{DC} is the DC-bias for the $n-$th LED array. Since $\mathbb{E}(x_n) = 0$, I_n^{DC} uniquely determines the average brightness of the LED arrays. Denote η as the LED conversion factor, the emitted optical power of the $n-$th LED array is given by $P_n^s = \eta u_n$. Let us define $\mathbf{P}^s = \left[P_1^s\ P_2^s\ \ldots\ P_{N_T}^s\right]^T$ as the LED arrays' emitted optical power vector. Then, the received optical power at the $k-$th user is expressed by

$$P_k^s = \mathbf{H}_k \mathbf{P}_k^s. \tag{7}$$

If we denote γ as the PD responsivity, the output electrical signal of the PD is then given by

$$\begin{aligned} y_k &= \gamma P_k^r + n_k = \gamma\eta \mathbf{H}_k \mathbf{u} + n_k \\ &= \gamma\eta \left(\mathbf{H}_k \mathbf{W}_k d_k + \underbrace{\mathbf{H}_k \sum_{i=1, i\neq k}^{K} \mathbf{W}_i d_i}_{\text{multi-user interference}} + \underbrace{\mathbf{H}_k \mathbf{I}^{\mathrm{DC}}}_{\text{DC current}} \right) \\ &\quad + \underbrace{n_k}_{\text{noise}}, \end{aligned} \tag{8}$$

where $\mathbf{u} = \left[u_1\ u_2\ \ldots\ u_{N_T}\right]^T$ and $\mathbf{I}^{\mathrm{DC}} = \left[I_1^{\mathrm{DC}}\ I_2^{\mathrm{DC}}\ \ldots\ I_{N_T}^{\mathrm{DC}}\right]^T$ are the transmitted signal vector and the DC-bias vector, respectively. In (8), $\mathbf{W}_k$ is the precoder for the $k-$th user and is given by $\mathbf{W}_k = \left[w_{1,k}\ w_{2,k}\ \ldots\ w_{N_T,k}\right]^T$. The receiver noise n_k component comprises shot noise and thermal noise and can be modeled as zero-mean Gaussian noise with variance σ_k^2 given by [3]

$$\sigma_k^2 = 2\gamma e \overline{P_k^r} B + 4\pi e A_r \gamma \chi_{\mathrm{amb}} (1 - \cos(\Psi)) B + i_{\mathrm{amp}}^2 B, \tag{9}$$

where e is the elementary charge, B denotes the system bandwidth and $\overline{P_k^r} = \mathbb{E}\left[P_k^r\right] = \eta \mathbf{H}_k \mathbf{I}^{\mathrm{DC}}$ is the average received optical power at the $k-$th user. i_{amp} is the pre-amplifier noise current density, χ_{amb} is the ambient light photocurrent. It is seen from (8) that the DC current term $\mathbf{H}_k \mathbf{I}^{\mathrm{DC}}$, which carries no information, can be removed by AC coupling. The information-carrying signal is then given by

$$y_k = \gamma\eta \left(\mathbf{H}_k \mathbf{W}_k d_k + \mathbf{H}_k \sum_{i=1, i\neq k}^{K} \mathbf{W}_i d_i \right) + n_k. \tag{10}$$

Since the AN vector is not necessarily orthogonal to the eavesdropper's channel matrix, the received signal at the eavesdropper contains both information-carrying and AN signals as

$$y_e = \gamma\eta \left(\mathbf{H}_e \sum_{i=1}^{K} \mathbf{W}_i d_i + \underbrace{\mathbf{H}_e (\boldsymbol{\rho} \circ \mathbf{G})\, \mathbf{z}}_{\text{AN}} \right) + \underbrace{n_e}_{\text{noise}}, \tag{11}$$

where $\mathbf{H}_e$ is the eavesdropper's channel matrix and $\boldsymbol{\rho} = \left[\rho_1\ \rho_2\ \ldots\ \rho_{N_T}\right]^T$.

2) ACTIVE EAVESDROPPER

It should be noted that the null-space approach in previous section is conservative in the sense that it limits the degrees of freedom in the AN design. In the case of active eavesdropper (i.e., the transmitters have the knowledge of the eavesdropper's CSI), the AN is not necessary to be orthogonal to the users' aggregate channel matrix. Instead, by knowing eavesdropper's CSI, the transmitters optimally design users' and AN's precoders to meet the fairness requirements on users' SINRs while keeping the SINR of the eavesdropper below a pre-described threshold. Fig. 3 illustrates the AN-aided precoding model in this case where $\widetilde{\mathbf{z}} = \left[\widetilde{z}_1\ \widetilde{z}_2\ \ldots\ \widetilde{z}_{N_T}\right]^T \in \mathbb{R}^{N_T \times 1}$ as the AN noise vector and $\widetilde{\mathbf{G}} \in \mathbb{R}^{N_T \times N_T}$ as its precoder, which can be an arbitrary matrix. Similar to the case of passive eavesdropper, each element $\widetilde{z}_i$ of $\widetilde{\mathbf{z}}$ is assumed to be zero mean and uniformly distributed over $[-1, 1]$.

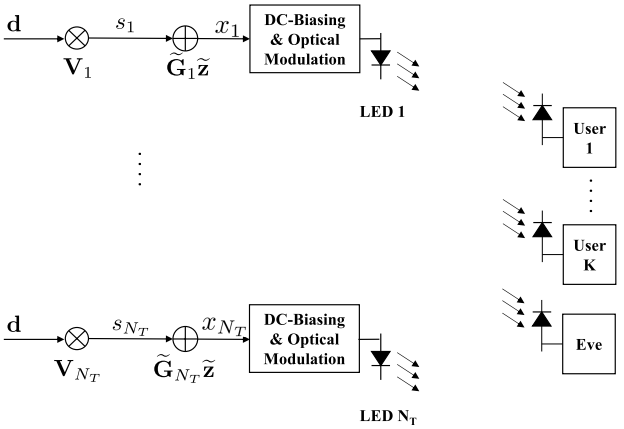

FIGURE 3. Schematic diagram of AN-aided precoding scheme: active eavesdropper.

The received signals at the $k-$th user and at the eavesdropper are then expressed by

$$y_k = \gamma\eta\left(\mathbf{H}_k\mathbf{W}_k d_k + \underbrace{\mathbf{H}_k\sum_{i=1,i\neq k}^{K}\mathbf{W}_i d_i}_{\text{multi-user interference}} + \underbrace{\mathbf{H}_k\widetilde{\mathbf{G}}\widetilde{\mathbf{z}}}_{\text{AN}}\right) + \underbrace{n_k}_{\text{noise}}, \tag{12}$$

and

$$y_e = \gamma\eta\left(\mathbf{H}_e\sum_{i=1}^{K}\mathbf{W}_i d_i + \underbrace{\mathbf{H}_e\widetilde{\mathbf{G}}\widetilde{\mathbf{z}}}_{\text{AN}}\right) + \underbrace{n_e}_{\text{noise}}, \tag{13}$$

respectively.

C. OPTICAL POWER CONSTRAINTS

Due to the nonlinear transfer characteristic of the LEDs, signal constraints in VLC are unique and fundamentally different from those of RF communications. Following the arguments described [10], to ensure normal and energy efficient operations of the LEDs, the drive current u_n must be constrained within a certain range $[0, I_{\max}]$, where a linear relationship between the drive current and the output optical power holds as illustrated in Fig. 4. The constraint is reflected in the following inequalities

$$0 \leq x_n + I_n^{\text{DC}} \leq I_{\max}. \tag{14}$$

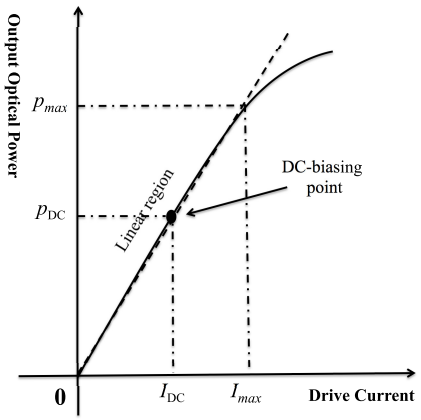

FIGURE 4. Nonlinear LED transfer characteristic.

For the case of passive eavesdropper, since the data symbol $|d_i|$ and the AN $|z_i|$ are constrained between $[-1, 1]$, we obtain

$$-\left(\|\mathbf{V}_n\|_1 + \rho_n\|\mathbf{G}_n\|_1\right) \leq x_n \leq \left(\|\mathbf{V}_n\|_1 + \rho_n\|\mathbf{G}_n\|_1\right). \tag{15}$$

Note that $\|\mathbf{V}_n\|_1 = \sum_{i=1}^{K}\|[\mathbf{W}_k]_n\|_1$ where $[\mathbf{W}_k]_n$ is the n-th row vector of $\mathbf{W}_k$. To ensure both (14) and (15) hold, one must consider the following constraint in the precoding design

$$\sum_{i=1}^{K}\|[\mathbf{W}_k]_n\|_1 + \rho_n\|\mathbf{G}_n\|_1 \leq \Delta_n, \tag{16}$$

with $\Delta_n = \min\left(I_n^{\text{DC}}, I_{\max} - I_n^{\text{DC}}\right)$.

By the same manner, the optical power constraint in the case of active eavesdropper is written as

$$\sum_{i=1}^{K}\|[\mathbf{W}_k]_n\|_1 + \|\widetilde{\mathbf{G}}_n\|_1 \leq \Delta_n, \tag{17}$$

where $\widetilde{\mathbf{G}}_n$ is the $n-$th row vector of $\widetilde{\mathbf{G}}$.

If we define $\mathbf{W} = \left[\mathbf{W}_1\ \mathbf{W}_2\ \ldots\ \mathbf{W}_K\right]$, the constraints in (16) and (17) can be equivalently represented by

$$\|[\mathbf{W}]_n\|_1 + \rho_n\|\mathbf{G}_n\|_1 \leq \Delta_n, \tag{18}$$

and

$$\|[\mathbf{W}]_n\|_1 + \|\widetilde{\mathbf{G}}_n\|_1 \leq \Delta_n, \tag{19}$$

respectively.

III. GENERAL AN-AIDED PRECODING DESIGNS

A. PASSIVE EAVESDROPPER

From (10) the SINR of the $k-$th legitimate user is given by

$$\text{SINR}_k = \frac{\theta^2\,|\mathbf{H}_k\mathbf{W}_k|^2}{\theta^2\sum\limits_{i=1,i\neq k}^{K}|\mathbf{H}_k\mathbf{W}_i|^2 + \sigma_k^2}, \tag{20}$$

where $\theta = \frac{1}{\sqrt{3}}\gamma\eta$. In the considered wiretap channel with K users, each of the K data symbols can be eavesdropped by the eavesdropper. Accordingly from (11), the SINR of the eavesdropper for the data symbol it eavesdrops on the $k-$th user is given by

$$\text{SINR}_{e,k} = \frac{\theta^2\,|\mathbf{H}_e\mathbf{W}_k|^2}{\theta^2\sum\limits_{i=1,i\neq k}^{K}|\mathbf{H}_e\mathbf{W}_i|^2 + \theta^2\,\|\mathbf{H}_e\,(\boldsymbol{\rho}\circ\mathbf{G})\|_F^2 + \sigma_e^2}, \tag{21}$$

In this passive eavesdropper scenario, the design strategy is to solve the users' SINR max-min fairness problem taking into account the optical power constraint in (16). The optimization problem is formulated as follows

$$\begin{aligned}\mathcal{P}1:\ &\underset{\mathbf{W}_k}{\text{maximize}}\ \min_k\ \text{SINR}_k\\ &\text{subject to}\ \sum_{i=1}^{K}\|[\mathbf{W}_k]_n\|_1 + \rho_n\,\|\mathbf{G}_n\|_1 \leq \Delta_n.\end{aligned} \tag{22}$$

It is noticed that the feasibility of $\mathcal{P}1$ depends on how to choose ρ_n's so that the inequality constraints hold. In principle, ρ_n's are set individually depending on the AN power allocated in each LED transmitter. In fact, setting ρ_n's individually can further improve the secrecy performance. For example, maximum AN power should be allocated to transmitters, which do not associate with any users. By doing so, the chance of degrading the eavesdropper's channel by AN can be considerably higher. However, for the sake of simplicity, we assume that ρ_n's are equal (i.e., $\rho_i = \rho_j = \rho$). Then, one can set $\rho = \frac{\overline{\rho}\min\Delta_n}{\max\|\mathbf{G}_n\|_1}$, where $\overline{\rho}$ $(0 \leq \overline{\rho} \leq 1)$ is a constant which controls the amplitude of the AN in the

sense that the larger the $\bar{p}$ is, the higher the AN amplitude (i.e., power) becomes. To solve $\mathcal{P}1$, it is necessary to introduce a slack variable t and reformulate the problem as follows

$$\begin{aligned}\mathcal{P}2: \ &\underset{\mathbf{W}_k,t}{\text{maximize}}\ t \\ &\text{subject to}\ \frac{|\mathbf{H}_k\mathbf{W}_k|^2}{\sum_{i=1,i\neq k}^{K}|\mathbf{H}_k\mathbf{W}_i|^2+\sigma_k'^2}\geq t \\ &\sum_{i=1}^{K}\|[\mathbf{W}_k]_n\|_1\leq\Delta_{\bar{\rho},n},\end{aligned}\tag{23}$$

where $\sigma_k'^2=\sigma_k^2/\theta^2$ and $\Delta_{\bar{\rho},n}=\Delta_n-\frac{\bar{\rho}\min\Delta_n}{\max\|\mathbf{G}_n\|_1}\|\mathbf{G}_n\|_1$. It can be seen that the objective function and the second constraint of the above problem are convex, yet the first constraint is not. To solve $\mathcal{P}2$, we first transform the non-convex constraint to be convex for a fixed value of t. Then, the bisection method is used to to solve the transformed optimization problem. Using the same variable transformations in [30], the two constraints in $\mathcal{P}2$ are equivalently represented by

$$\left\|\mathbf{B}_k\mathbf{w}+\boldsymbol{\sigma}'_k\right\|_F\leq\frac{1}{\sqrt{t}}\mathbf{H}_k(\mathbf{I}_{N_T}\otimes\mathbf{e}_k^T)\mathbf{w}\tag{24}$$

$$-\mathbf{a}\leq\mathbf{w}\leq\mathbf{a},\tag{25}$$

$$\mathbf{U}\mathbf{a}\leq\boldsymbol{\Delta}_{\bar{\rho}},\tag{26}$$

where $\mathbf{w}=\text{vec}(\mathbf{W}^T)$ and $\mathbf{I}_K^k$ be the matrix obtained from the identity matrix of size K by setting the $(k,k)-$th element be zero, $\mathbf{B}_k=\begin{bmatrix}\mathbf{H}_k\otimes\mathbf{I}_K^k\\ \mathbf{0}_{1\times N_TK}\end{bmatrix}$, $\boldsymbol{\sigma}'_k=\begin{bmatrix}\mathbf{0}_{1\times K}\ \sigma'_k\end{bmatrix}^T$, $\mathbf{U}=\mathbf{I}_{N_T}\otimes\mathbf{1}_K^T$, $\boldsymbol{\Delta}_{\bar{\rho}}=\begin{bmatrix}\Delta_{\bar{\rho},1}\ \Delta_{\bar{\rho},2}\ \dots\ \Delta_{\bar{\rho},N_T}\end{bmatrix}^T$, and $\mathbf{a}=\begin{bmatrix}a_1\ a_2\ \dots\ a_{N_TK}\end{bmatrix}^T$ is a new optimization variable. The next step is to solve the following feasibility problem with respect to $\mathbf{w}$

$$\begin{aligned}\mathcal{P}3: \ &\text{find}\ \mathbf{w} \\ &\text{subject to}\ \left\|\mathbf{B}_k\mathbf{w}+\boldsymbol{\sigma}'_k\right\|_F\leq\frac{1}{\sqrt{t}}\mathbf{H}_k(\mathbf{I}_{N_T}\otimes\mathbf{e}_k^T)\mathbf{w} \\ &-\mathbf{a}\leq\mathbf{w}\leq\mathbf{a}, \\ &\mathbf{U}\mathbf{a}\leq\boldsymbol{\Delta}_{\bar{\rho}},\end{aligned}\tag{27}$$

It is obvious that the above problem is a second-order cone program (SOCP) [33]. Thus, standard optimization packages, such as CVX or YAMIP [36], [37], can be used to solve the problem efficiently. Finally, based on the observation that the solution to $\mathcal{P}2$ is the maximum value of t at which $\mathcal{P}3$ is feasible, the bisection algorithm as described in detail in [30] can be utilized to find the optimal solution. The algorithm is presented here for the sake of convenience.

Algorithm 1 Bisection Algorithm for Solving Problem $\mathcal{P}2$

1) Initialize t_1 and t_2 ($t_1 < t_2$) so that $\mathcal{P}3$ is infeasible when $t=t_2$ and feasible when $t=t_1$.
2) Define a tolerance parameter τ.

while $t_2-t_1>\tau$ **do**
  $t=(t_1+t_2)/2$.
  Solve the feasibility of $\mathcal{P}3$ by CVX toolbox.
  if the problem is feasible **then** $t_1=t$.
  else $t_2=t$.
  end if
end while
The optimal precoder $\mathbf{W}_k^*$ is given by $\mathbf{W}_k^*=(\mathbf{I}_{N_T}\otimes\mathbf{e}_k^T)\widetilde{\mathbf{w}}$, where $\widetilde{\mathbf{w}}$ is the solution to $\mathcal{P}3$ with $t=t_1$.

B. ACTIVE EAVESDROPPER

Following (12) and (13), the SINRs of the $k-$th legitimate user and the eavesdropper are given by

$$\text{SINR}_k=\frac{|\mathbf{H}_k\mathbf{W}_k|^2}{\sum_{i=1,i\neq k}^{K}|\mathbf{H}_k\mathbf{W}_i|^2+\left\|\mathbf{H}_k\widetilde{\mathbf{G}}\right\|_F^2+\sigma_k'^2},\tag{28}$$

and

$$\text{SINR}_{e,k}=\frac{|\mathbf{H}_e\mathbf{W}_k|^2}{\sum_{i=1,i\neq k}^{K}|\mathbf{H}_e\mathbf{W}_i|^2+\left\|\mathbf{H}_e\widetilde{\mathbf{G}}\right\|_F^2+\sigma_e'^2},\tag{29}$$

respectively, where $\sigma_e'^2=\sigma_e^2/\theta^2$. Different from the passive scenario, the availability of the eavesdropper's CSI enables the transmitters to control the SINR performance of the eavesdropper via designing AN. More specifically, the AN is designed to limit the eavesdropper's SINRs below certain thresholds. As such, the max-min fairness problem is formulated as follows

$$\begin{aligned}\mathcal{P}4: \ &\underset{\mathbf{W}_k,\widetilde{\mathbf{G}}}{\text{maximize}}\ \min_k\ \text{SINR}_k \\ &\text{subject to}\ \text{SINR}_{e,k}\leq\lambda_k, \\ &\sum_{i=1}^{K}\|[\mathbf{W}_k]_n\|_1+\left\|\widetilde{\mathbf{G}}_n\right\|_1\leq\Delta_n,\end{aligned}\tag{30}$$

where λ_k is the threshold for $\text{SINR}_{e,k}$. It should be noted that it is crucial to choose the thresholds so that large differences between users' and eavesdropper's SINR could be guaranteed. On the other hand, if λ_k's are set too low (i.e., too demanding constraints on the eavesdropper's SINRs), the optimization problem may not be feasible. In addition, adaptive selections of λ_k's to optimize the fairness performance are also important due to users and eavesdropper channel variations. This is, however, beyond the scope of the study. Compared to $\mathcal{P}1$, it is obvious that the above optimization problem is more difficult to solve due to the additional non-convex constraints on the eavesdropper's SINRs. Moreover, the problem involves a joint design of both users's precoders $\mathbf{W}_k$ and the AN's precoder $\widetilde{\mathbf{G}}$. Following the same procedure as in the case of passive eavesdropper, firstly, we rewrite $\mathcal{P}4$ to the an equivalent form as follows

$$\begin{aligned}\mathcal{P}5: \ &\underset{\mathbf{W}_k,\widetilde{\mathbf{G}},t}{\text{maximize}}\ t \\ &\text{subject to}\ \text{SINR}_k\geq t, \\ &\text{SINR}_{e,k}\leq\lambda_k, \\ &\sum_{i=1}^{K}\|[\mathbf{W}_k]_n\|_1+\left\|\widetilde{\mathbf{G}}_n\right\|_1\leq\Delta_n.\end{aligned}\tag{31}$$

By the same manner as in the previous section, the constraints of $\mathcal{P}5$ can be reformulated as follows

$$\left\|\mathbf{B}_k\mathbf{q}+\boldsymbol{\sigma}'_k\right\|_F \le \frac{1}{\sqrt{t}}\mathbf{H}_k\left(\mathbf{I}_{N_T}\otimes(\mathbf{e}_k^T\mathbf{V})\right)\mathbf{q}, \quad (32)$$

$$\left\|\mathbf{B}_{e,k}\mathbf{q}+\boldsymbol{\sigma}'_e\right\|_F \ge \frac{1}{\sqrt{\lambda_k}}\mathbf{H}_e\left(\mathbf{I}_{N_T}\otimes(\mathbf{e}_k^T\mathbf{V})\right)\mathbf{q}, \quad (33)$$

$$-\mathbf{a} \le \mathbf{q} \le \mathbf{a}, \quad (34)$$

$$\mathbf{U}\mathbf{a} \le \boldsymbol{\Delta}, \quad (35)$$

where $\mathbf{W} = \left[\mathbf{W}_1\ \mathbf{W}_2\ \dots\ \mathbf{W}_K\right]$, $\mathbf{Q} = \left[\mathbf{W}\ \widetilde{\mathbf{G}}\right] \in \mathbb{R}^{N_T\times(N_T+K)}$, and $\mathbf{q} = \mathrm{vec}\left(\mathbf{Q}^T\right)$. $\mathbf{B}_k = \begin{bmatrix}\mathbf{H}_k\otimes\mathbf{I}^k_{N_T+K}\\ \mathbf{0}_{1\times N_T(N_T+K)}\end{bmatrix}$, $\mathbf{B}_{e,k} = \begin{bmatrix}\mathbf{H}_e\otimes\mathbf{I}^k_{N_T+K}\\ \mathbf{0}_{1\times N_T(N_T+K)}\end{bmatrix}$, $\mathbf{V} = \left[\mathbf{I}_K\ \mathbf{0}_{K\times N_T}\right]$, $\mathbf{U} = \mathbf{I}_{N_T}\otimes\mathbf{1}^T_{N_T+K}$, $\boldsymbol{\Delta} = \left[\Delta_1\ \Delta_2\ \dots\ \Delta_{N_T}\right]^T$, $\boldsymbol{\sigma}'_k = \left[\mathbf{0}_{1\times(N_T+K)}\ \sigma'_k\right]^T$, $\boldsymbol{\sigma}'_e = \left[\mathbf{0}_{1\times(N_T+K)}\ \sigma'_e\right]^T$, and $\mathbf{a} = \left[a_1\ a_2\ \dots\ a_{N_T(N_T+K)}\right]^T$. Now, for a fixed value of t, we solve the feasibility of the following problem with respect to $\mathbf{q}$

$$\begin{aligned}\mathcal{P}6:\ &\text{find } \mathbf{q}\\ &\text{subject to } \left\|\mathbf{B}_k\mathbf{q}+\boldsymbol{\sigma}'_k\right\|_F \le \frac{1}{\sqrt{t}}\mathbf{H}_k\left(\mathbf{I}_{N_T}\otimes(\mathbf{e}_k^T\mathbf{V})\right)\mathbf{q},\\ &\left\|\mathbf{B}_{e,k}\mathbf{q}+\boldsymbol{\sigma}'_e\right\|_F\\ &\ge \frac{1}{\sqrt{\lambda_k}}\mathbf{H}_e\left(\mathbf{I}_{N_T}\otimes(\mathbf{e}_k^T\mathbf{V})\right)\mathbf{q},\\ &-\mathbf{a}\le\mathbf{q}\le\mathbf{a},\\ &\mathbf{U}\mathbf{a}\le\boldsymbol{\Delta}. \quad (36)\end{aligned}$$

It can be seen that the second constraint of the above problem is still not convex. Thus, further transformations are needed to reformulate $\mathcal{P}6$ to a convex optimization problem. In this paper, we adopt the convex-concave procedure (CCCP) to solve $\mathcal{P}6$ [31], [32]. The basic idea of the CCCP is to approximate a nonconvex problem by a convex one and iteratively solve the approximating problem until the optimal solution converges with a satisfactory error. Specifically for $\mathcal{P}6$, at each iteration, we approximately linearize the Frobenius term $\left\|\mathbf{B}_{e,k}\mathbf{q}+\boldsymbol{\sigma}'_e\right\|_F$ using its Taylor expansion as $\left\|\mathbf{B}_{e,k}\mathbf{q}^{(i)}+\boldsymbol{\sigma}'_e\right\|_F \approx \left\|\mathbf{B}_{e,k}\mathbf{q}^{(i-1)}+\boldsymbol{\sigma}'_e\right\|_F + \frac{\left[\mathbf{B}_{e,k}\mathbf{q}^{(i-1)}+\boldsymbol{\sigma}'_e\right]^T\mathbf{B}_{e,k}}{\left\|\mathbf{B}_{e,k}\mathbf{q}^{(i-1)}+\boldsymbol{\sigma}'_e\right\|_F}\left(\mathbf{q}^{(i)}-\mathbf{q}^{(i-1)}\right)$, where $\mathbf{q}^{(i-1)}$ is the value of $\mathbf{q}$ obtained from the previous iteration. Replacing the approximating term to the second constraint, $\mathcal{P}6$ is approximated to a convex optimization problem $\mathcal{P}7$, which is on the bottom of this page. The detailed CCCP for solving $\mathcal{P}6$ is given in **Algorithm 2**.

Algorithm 2 CCCP for Solving Problem $\mathcal{P}6$

1: **Initialization**
   1) Initialize $\mathbf{q}^{(0)}$ to be sufficiently small to ensure $\mathcal{P}7$ is feasible.
   2) Maximum number of iterations $L = 10$ and convergence error $\epsilon = 10^{-3}$.

2: **Iteration**: At the $i-$th iteration
   1) Solving $\mathcal{P}7$ using the CVX toolbox to get $\mathbf{q}^{(i)}$ given $\mathbf{q}^{(i-1)}$ obtained from previous iteration.
   2) $i = i+1$.

3: **Termination**: terminate the iteration when one of the two following criteria is met
   1) $\left\|\mathbf{q}^{(i)}-\mathbf{q}^{(i-1)}\right\|_F \le \epsilon$ or $i = L$.

Once $\mathcal{P}6$ is solved, the solution to $\mathcal{P}5$ can be found by using the bisection method as described in **Algorithm 1**.

IV. AN-AIDED PRECODING DESIGNS USING ZF

In this section, specific designs for the proposed AN-aided precoding scheme using ZF technique are described. ZF aims at decoupling the multi-user channel into multiple independent subchannels, thus simplifies the AN design. Moreover, this independency among subchannels naturally results in the confidentiality among users. Mathematically speaking, ZF precoding constructs the precoder $\mathbf{W}_i$ of the $i-$th user in such a way that it is orthogonal to channel matrices of other users, that is

$$\mathbf{H}_k\mathbf{W}_i = 0 \quad \forall k \ne i. \quad (38)$$

For mathematical connivence, we can express the above equations in a more compact form as follows

$$\mathbf{H}\mathbf{W} = \begin{bmatrix}\sqrt{p_1} & & & \\ & \sqrt{p_2} & & \\ & & \ddots & \\ & & & \sqrt{p_K}\end{bmatrix} = \mathrm{diag}\{\sqrt{\mathbf{p}}\}, \quad (39)$$

where $\sqrt{\mathbf{p}} = \left[\sqrt{p_1}\ \sqrt{p_2}\ \dots\ \sqrt{p_K}\right]^T \in \mathbb{R}^{1\times K}$ representing users' channel gains. $\mathbf{W}$ can then be written in the following

$$\begin{aligned}\mathcal{P}7:\ &\text{find } \mathbf{q}^{(i)}\\ &\text{subject to } \left\|\mathbf{B}_k\mathbf{q}^{(i)}+\boldsymbol{\sigma}'_k\right\|_F \le \frac{1}{\sqrt{t}}\mathbf{H}_k\left(\mathbf{I}_{N_T}\otimes(\mathbf{e}_k^T\mathbf{V})\right)\mathbf{q}^{(i)},\\ &\left\|\mathbf{B}_{e,k}\mathbf{q}^{(i-1)}+\boldsymbol{\sigma}'_e\right\|_F + \frac{\left[\mathbf{B}_{e,k}\mathbf{q}^{(i-1)}+\boldsymbol{\sigma}'_e\right]^T\mathbf{B}_{e,k}}{\left\|\mathbf{B}_{e,k}\mathbf{q}^{(i-1)}+\boldsymbol{\sigma}'_e\right\|_F}\left(\mathbf{q}^{(i)}-\mathbf{q}^{(i-1)}\right) \ge \frac{1}{\sqrt{\lambda_k}}\mathbf{H}_e\left(\mathbf{I}_{N_T}\otimes(\mathbf{e}_k^T\mathbf{V})\right)\mathbf{q}^{(i)},\\ &-\mathbf{a}\le\mathbf{q}^{(i)}\le\mathbf{a},\\ &\mathbf{U}\mathbf{a}\le\boldsymbol{\Delta}. \quad (37)\end{aligned}$$

form

$$\mathbf{W} = \mathbf{H}^{-}\text{diag}\{\sqrt{\mathbf{p}}\}, \tag{40}$$

where $\mathbf{H}^{-}$ is the generalized inverse of $\mathbf{H}$, which can be any matrix that satisfies $\mathbf{H}\mathbf{H}^{-}\mathbf{H} = \mathbf{H}$. Generally, with the assumption that $\mathbf{H}$ is full row-rank, any generalized inverses $\mathbf{H}^{-}$ can be expressed by

$$\mathbf{H}^{-} = \mathbf{H}^{\dagger} + \mathbf{P}\mathbf{Q}, \tag{41}$$

where $\mathbf{H}^{\dagger} = \mathbf{H}^{T}(\mathbf{H}\mathbf{H}^{T})^{-1}$ is the pseudo-inverse of $\mathbf{H}$, $\mathbf{P} = \mathbf{I} - \mathbf{H}^{\dagger}\mathbf{H}$ is the projection onto the null space of $\mathbf{H}$ and $\mathbf{Q}$ is an arbitrary matrix. Then, the general structure of any ZF precoding matrix $\mathbf{W}$ is given by

$$\mathbf{W} = \left[\mathbf{H}^{\dagger} + \mathbf{P}\mathbf{Q}\right]\text{diag}\{\sqrt{\mathbf{p}}\}. \tag{42}$$

With this expression, the AN design problems reduce to optimization problems with respect to $\mathbf{p}$ and the choice of $\mathbf{Q}$.

A. PASSIVE EAVESDROPPER

With ZF precoding, the SINR of the $k-$th user is given by

$$\text{SINR}_k^{\text{ZF}} = \frac{|\mathbf{H}_k\mathbf{W}_k|^2}{\sigma_k'^2} = \frac{p_k}{\sigma_k'^2}, \tag{43}$$

Taking the ZF constraint in (39), the max-min fairness problem is formulated as

$$\begin{aligned}\mathcal{P}8: \ &\underset{\mathbf{W}_k}{\text{maximize}} \ \min_k \frac{p_k}{\sigma_k'^2}\\ &\text{subject to } \mathbf{H}\mathbf{W} = \text{diag}\{\sqrt{\mathbf{p}}\},\\ &\sum_{i=1}^{K}\|[\mathbf{W}_k]_n\|_1 + \rho_n\|\mathbf{G}_n\|_1 \le \Delta_n. \end{aligned}\tag{44}$$

Similar to the case of general design, we assume that ρ_n's are set equally at all LED transmitters. Let us define $\boldsymbol{\sigma}'^2 = \left[\sigma_1'^2\ \sigma_2'^2\ \dots\ \sigma_K'^2\right]^T$ and $\text{diag}\{\mathbf{p}'\} = \text{diag}\{\mathbf{p}\}\text{diag}\{\boldsymbol{\sigma}'^2\}$ where $\mathbf{p}' = \left[p_1'\ p_2'\ \dots\ p_K'\right]$. Then, $\mathcal{P}8$ can be rewritten as

$$\begin{aligned}\mathcal{P}9: \ &\underset{\mathbf{W}_k}{\text{maximize}} \ \min_k p_k'\\ &\text{subject to } \mathbf{H}\mathbf{W} = \text{diag}\{\sqrt{\mathbf{p}'}\}\text{diag}\{\boldsymbol{\sigma}'\},\\ &\|[\mathbf{W}]_n\|_1 \le \Delta_{\overline{\rho},n}. \end{aligned}\tag{45}$$

In the above problem, the optical power constraint has been rewritten with respect to $\mathbf{W}$. Following the similar argument in [34], the optimal solution to $\mathcal{P}9$ is in the form $\mathbf{p}' = p'\mathbf{1}$ for some p' is optimal. In order to proof this, let $\mathbf{W}^*$ and $\mathbf{p}^*$ be the optimal solution to the problem and we define new variables $\mathbf{p}' = \overline{p}\mathbf{1}$ and $\mathbf{W} = \mathbf{W}^*\text{diag}\left\{\left[\sqrt{\overline{p}/p_1^*}\ \dots\ \sqrt{\overline{p}/p_K^*}\right]\right\}$, where $\overline{p} = \min_k p_k^*$. Then, it holds that

$$\begin{aligned}\mathbf{H}\mathbf{W} &= \mathbf{H}\mathbf{W}^*\text{diag}\left\{\left[\sqrt{\overline{p}/p_1^*}\ \dots\ \sqrt{\overline{p}/p_K^*}\right]\right\}\\ &= \text{diag}\{\sqrt{\mathbf{p}^*}\}\text{diag}\{\sqrt{\boldsymbol{\sigma}}\}\text{diag}\left\{\left[\sqrt{\overline{p}/p_1^*}\ \dots\ \sqrt{\overline{p}/p_K^*}\right]\right\}\\ &= \text{diag}\{\sqrt{\mathbf{p}'}\}\text{diag}\{\sqrt{\boldsymbol{\sigma}}\}, \end{aligned}\tag{46}$$

and

$$\begin{aligned}\|[\mathbf{W}]_n\|_1 &= \left\|\left[\mathbf{W}^*\text{diag}\left\{\left[\sqrt{\overline{p}/p_1^*}\ \dots\ \sqrt{\overline{p}/p_K^*}\right]\right\}\right]_n\right\|_1\\ &\le \|[\mathbf{W}^*]_n\|_1, \end{aligned}\tag{47}$$

since $\overline{p}/p_k^* \le 1$ for all k. That is, $\mathbf{W}$ and $\mathbf{p}'$ are also feasible and offer the same objective. We thus can reduce $\mathcal{P}9$ to

$$\begin{aligned}\mathcal{P}10: \ &\underset{p'\ge 0,\mathbf{Q}}{\text{maximize}} \ p'\\ &\text{subject to } \sqrt{p'\sigma_n^2}\left\|\left[\mathbf{H}^{\dagger} + \mathbf{P}\mathbf{Q}\right]_n\right\|_1 \le \Delta_{\overline{\rho},n}. \end{aligned}$$

It is easy to see that the optimal solution p_{opt}' is given by

$$p_{\text{opt}}' = \min_n \frac{\Delta_{\overline{\rho},n}^2}{\sigma_n'\left\|\left[\mathbf{H}^{\dagger} + \mathbf{P}\mathbf{Q}\right]_n\right\|_1^2}, \tag{48}$$

where $\mathbf{Q}$ is the solution to

$$\begin{aligned}\mathcal{P}11: \ &\underset{\mathbf{Q},t}{\text{minimize}} \ t\\ &\text{subject to } \sigma_n'\left\|\left[\mathbf{H}^{\dagger} + \mathbf{P}\mathbf{Q}\right]_n\right\|_1^2 \le t. \end{aligned}$$

The above problem is a linear programming, which has been well studied in literature [35].

B. ACTIVE EAVESDROPPER

In this case, the SINR of the $k-$ user is simplified as

$$\text{SINR}_k^{\text{ZF}} = \frac{|\mathbf{H}_k\mathbf{W}_k|^2}{\left\|\mathbf{H}_k\widetilde{\mathbf{G}}\right\|_F^2 + \sigma_k'^2}. \tag{49}$$

Since ZF is only applied to legitimate users, the expression for the SINR of the eavesdropper is the same to that in (29). The max-min fairness problem is then given by

$$\begin{aligned}\mathcal{P}12: \ &\underset{\mathbf{W}_k,\widetilde{\mathbf{G}}}{\text{maximize}} \ \min_k \text{SINR}_k^{\text{ZF}}\\ &\text{subject to } \text{SINR}_{e,k}^{\text{ZF}} \le \lambda_k,\\ &\mathbf{H}_i\mathbf{W}_k = 0 \quad \forall k \ne i,\\ &\sum_{i=1}^{K}\|[\mathbf{W}_k]_n\|_1 + \left\|\widetilde{\mathbf{G}}_n\right\|_1 \le \Delta_n, \end{aligned}\tag{50}$$

It can be seen that it is difficult to handle the above problem by using of the expression in (42) due to the involvement of $\widetilde{\mathbf{G}}$ in both objective function and constraints. Instead, we follow the same procedure as in the case of the general design described in Section III. B to reformulate $\mathcal{P}11$ to a convex optimization problem. With the same variable transformations as in $\mathcal{P}6$, we solve the feasibility of the following problem

$$\begin{aligned}\mathcal{P}13: \ &\text{find } \mathbf{q}\\ &\text{subject to } \left\|\mathbf{B}_k\mathbf{q} + \boldsymbol{\sigma}'_k\right\|_F \le \frac{1}{\sqrt{t}}\mathbf{H}_k\left(\mathbf{I}_{N_T}\otimes(\mathbf{e}_k^T\mathbf{V})\right)\mathbf{q},\\ &\left\|\mathbf{B}_{e,k}\mathbf{q} + \boldsymbol{\sigma}'_e\right\|_F\\ &\ge \frac{1}{\sqrt{\lambda_k}}\mathbf{H}_e\left(\mathbf{I}_{N_T}\otimes(\mathbf{e}_k^T\mathbf{V})\right)\mathbf{q}, \end{aligned}$$

$$\begin{aligned}&\mathbf{H}_k\left(\mathbf{I}_{N_T}\otimes(\mathbf{e}_i^T\mathbf{V})\right)\mathbf{q}=0,\quad \forall k\neq i,\\&-\mathbf{a}\leq\mathbf{q}\leq\mathbf{a},\\&\mathbf{U}\mathbf{a}\leq\boldsymbol{\Delta}.\end{aligned}\tag{51}$$

Similar to $\mathcal{P}6$, the CCCP can be used to solve the above problem.

V. NUMERICAL RESULTS AND DISCUSSIONS

In this section, numerical examples are provided to compare the secrecy performances of the two AN-aided precoding designs presented in previous sections. The geographical configuration of the considered system, which consists of 4 LED arrays, is shown in Fig. 1. We assume that legitimate users and the eavesdropper are located on a receive plane, which is 0.5 m above the floor. For the position specification, a Cartesian coordinate system whose the origin is the center of the floor is used. In addition, all simulation results are obtained by averaging 5, 000 different channel realizations (i.e., 5, 000 different positions of legitimate users and eavesdropper uniformly placed on the receive plane). For the sake of conciseness, simulation results are illustrated for the case of 2 legitimate users. Furthermore, assume that the DC-bias I_n^{DC} are the same for all LED arrays (i.e., $I_i^{\mathrm{DC}}=I_j^{\mathrm{DC}}=I_0^{\mathrm{DC}}$). Unless otherwise noted, the parameters of the room, LED arrays and optical receivers are given in Table 1.

For the passive eavesdropper scenario, Fig. 5 presents the SINR performances of legitimate users and the eavesdropper

TABLE 1. System parameters.

Room and LED configurations	
Room dimension (Length × Width × Height)	5 (m) × 5 (m) × 3 (m)
LED array positions	array 1 : $(-\sqrt{2},-\sqrt{2},3)$ array 2 : $(\sqrt{2},-\sqrt{2},3)$ array 3 : $(\sqrt{2},\sqrt{2},3)$ array 4 : $(-\sqrt{2},\sqrt{2},3)$
LED bandwidth, B	20 MHz
LED beam angle, ϕ (LED Lambertian order is 1)	120°
LED conversion factor, η	0.44 W/A
Receiver photodetectors	
Active area, A_r	1 cm^2
Responsivity, γ	0.54 A/W
Field of view (FOV), Ψ	60°
Optical filter gain, $T_s(\psi)$	1
Refractive index of the concentrator, κ	1.5
Other parameters	
Ambient light photocurrent, χ_{amp}	10.93 A/(m$^2\cdot$ Sr)
Preamplifier noise current density, i_{amp}	5 pA/Hz$^{-1/2}$

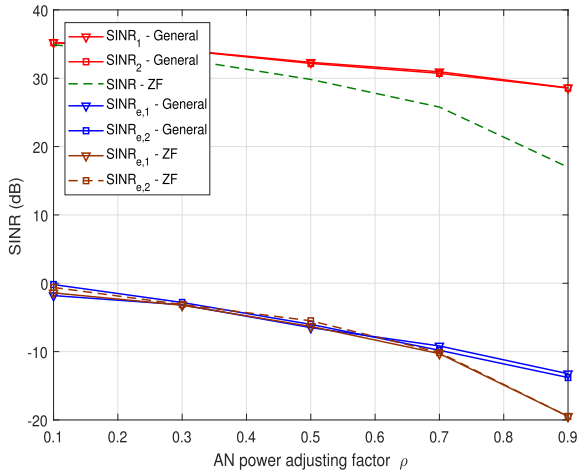

FIGURE 5. Users' and eavesdropper's SINRs versus $\overline{\rho}$: passive eavesdropper.

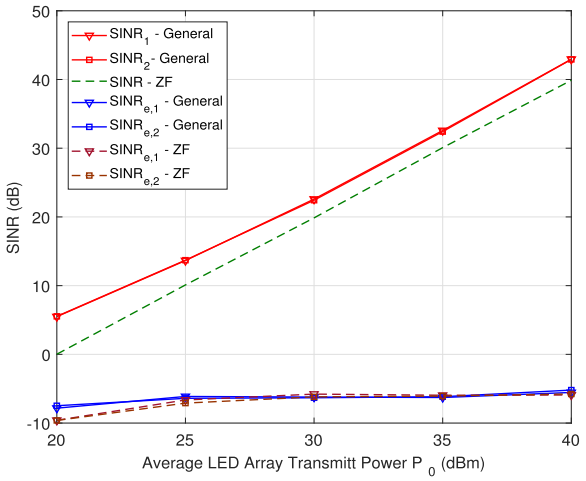

FIGURE 6. Users' and eavesdropper's SINRs versus average LED array transmit power: passive eavesdropper.

with respect to the AN power adjusting factor $\overline{\rho}$. The average LED array power $P_0=\mu I_0^{\mathrm{DC}}$ is set to 35 dBm. As we showed in Section IV.A that the ZF design has the optimal solution where users' SINR are equal. It also holds in the case of general design as numerically illustrated in the figure. We also observed that significant gaps between users' and eavesdropper's SINRs are achieved in both designs, thus ensuring high secrecy capacity performances. For example at $\rho=0.9$, the performance gaps are 40 dB and 36 dB in case of general and ZF designs, respectively.

In Fig. 6, the fairness performances versus average LED transmit power are illustrated. The AN power adjusting factor $\rho=0.5$ is set. It is seen that the general design, which optimizes users' SIRNs output, outperforms the ZF one, especially at lower transmit power. At high transmit power regimes, the performance of the ZF design approaches that of the general one. This reflects the fact that ZF precoding achieves good performance at high transmit power [34]. It is

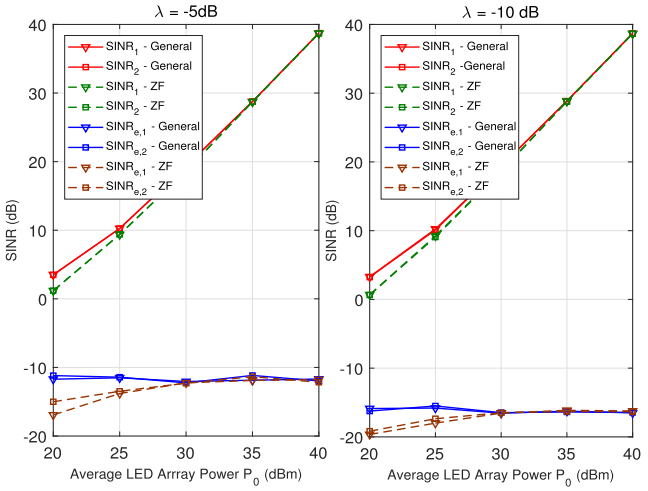

FIGURE 7. Users' and eavesdropper's SINRs versus average LED array transmit power: active eavesdropper.

also seen that the eavesdropper's SINRs in case of ZF design are lower than those of the general one at the low transmit power region. However, they are almost the same when the LED transmit power increases.

For the case of active eavesdropper, Fig. 7 depicts the max-min fairness performances in accordance with the average LED transmit power for different values of eavesdropper's SINR threshold. For simplicity, assume that λ_k's are set equal ($\lambda_k = \lambda_j = \lambda$). Specifically, we choose $\lambda = -5$ and -10 dB for simulations. Similar to the case of unknown $\mathbf{H}_e$, we also observed significant gaps between users' and eavesdropper' SINR in both general and ZF designs. Interestingly, while the eavesdropper's SINRs are kept almost constant in case of general design, they increase according to an increase in the transmit power in case of ZF design. Moreover, it is seen that users' performances in case $\lambda = -10$ dB are negligibly worse than those when a more relaxing threshold $\lambda = -5$ dB is imposed on the eavesdropper's SINR.

VI. CONCLUSIONS

In this paper, we have studied AN-aided precoding designs with respect to users' and eavesdropper's SINR performances for a multi-user VLC wiretap channels. In the case of passive eavesdropper, the AN was designed to lie on the null-space of the users' aggregate channel matrix. When the eavesdropper is active, the design aimed at limiting the eavesdropper's SINR below a certain threshold. A specific AN design, which utilizes ZF was also examined. In the former scenario, numerical results showed that, for the both designs (i.e., general and ZF), significant gaps between users' and eavesdropper's SINR were achieved. In the scenario of active eavesdropper and general design, it was observed that, the eavesdropper' SINRs were kept almost constant regardless of the transmitted power. In case of ZF design, the eavesdropper's SINR increased in accordance to an increase of the transmitted power. Similar to the case of unknown eavesdropper's CSI, both designs provided a sufficient secrecy level.

REFERENCES

[1] P. H. Pathak, X. Feng, P. Hu, and P. Mohapatra, "Visible light communication, networking, and sensing: A survey, potential and challenges," *IEEE Commun. Surveys Tuts.*, vol. 17, no. 4, pp. 2047–2077, 4th Quart., 2015.
[2] A. Jovicic, J. Li, and T. Richardson, "Visible light communication: Opportunities, challenges and the path to market," *IEEE Commun. Mag.*, vol. 51, no. 12, pp. 26–32, Dec. 2013.
[3] L. Zeng *et al.*, "High data rate multiple input multiple output (MIMO) optical wireless communications using white led lighting," *IEEE J. Sel. Areas Commun.*, vol. 27, no. 9, pp. 1654–1662, Dec. 2009.
[4] T. Fath and H. Haas, "Performance comparison of MIMO techniques for optical wireless communications in indoor environments," *IEEE Trans. Commun.*, vol. 61, no. 2, pp. 733–742, Feb. 2013.
[5] L. Wu, Z. Zhang, and H. Liu, "MIMO-OFDM visible light communications system with low complexity," in *Proc. IEEE Int. Conf. Commun. (ICC)*, Jun. 2013, pp. 3933–3937.
[6] A. Burton, H. L. Minh, Z. Ghassemlooy, E. Bentley, and C. Botella, "Experimental demonstration of 50-Mb/s visible light communications using 4 × 4 MIMO," *IEEE Photon. Technol. Lett.*, vol. 26, no. 9, pp. 945–948, May 1, 2014.
[7] A. Nuwanpriya, S.-W. Ho, and C. S. Chen, "Indoor MIMO visible light communications: Novel angle diversity receivers for mobile users," *IEEE J. Sel. Areas Commun.*, vol. 33, no. 9, pp. 1780–1792, Sep. 2015.
[8] H. Ma, L. Lampe, and S. Hranilovic, "Coordinated broadcasting for multiuser indoor visible light communication systems," *IEEE Trans. Commun.*, vol. 63, no. 9, pp. 3313–3324, Sep. 2015.
[9] B. Li, J. Wang, R. Zhang, H. Shen, C. Zhao, and L. Hanzo, "Multiuser MISO transceiver design for indoor downlink visible light communication under per-LED optical power constraints," *IEEE Photon. J.*, vol. 7, no. 4, Aug. 2015, Art. no. 7201415.
[10] T. V. Pham, H. Le-Minh, and A. T. Pham, "Multi-user visible light communication broadcast channels with zero-forcing precoding," *IEEE Trans. Commun.*, vol. 64, no. 6, pp. 2509–2521, Jun. 2017.
[11] A. Mukherjee, S. A. A. Fakoorian, J. Huang, and A. L. Swindlehurst, "Principles of physical layer security in multiuser wireless networks: A survey," *IEEE Commun. Surveys Tuts.*, vol. 16, no. 3, pp. 1550–1573, 3rd Quart., 2014.
[12] A. D. Wyner, "The wire-tap channel," *Bell Syst. Tech. J.*, vol. 54, no. 8, pp. 1355–1387, 1975.
[13] I. Csiszár and J. Korner, "Broadcast channels with confidential messages," *IEEE Trans. Inf. Theory*, vol. 24, no. 3, pp. 339–348, May 1978.
[14] S. Leung-Yan-Cheong and M. E. Hellman, "The Gaussian wire-tap channel," *IEEE Trans. Inf. Theory*, vol. IT-24, no. 4, pp. 451–456, Jul. 1978.
[15] A. Mostafa and L. Lampe, "Physical-layer security for MISO visible light communication channels," *IEEE J. Sel. Areas Commun.*, vol. 33, no. 9, pp. 1806–1818, Sep. 2015.
[16] S. Ma, Z. L. Dong, H. Li, Z. Lu, and S. Li, "Optimal and robust secure beamformer for indoor MISO visible light communication," *J. Lightw. Technol.*, vol. 34, no. 21, pp. 4988–4998, Nov. 1, 2016.
[17] A. Mostafa and L. Lampe, "Optimal and robust beamforming for secure transmission in MISO visible-light communication links," *IEEE Trans. Signal Process.*, vol. 64, no. 24, pp. 6501–6516, Dec. 2016.
[18] T. V. Pham and A. T. Pham, "Secrecy sum-rate of multi-user MISO visible light communication systems with confidential messages," *Optik*, vol. 151, pp. 65–76, Dec. 2017.
[19] S. Cho, G. Chen, and J. P. Coon, "Securing visible light communication systems by beamforming in the presence of randomly distributed eavesdroppers," *IEEE Trans. Wireless Commun.*, vol. 17, no. 5, pp. 2918–2931, May 2018.
[20] X. Zhao, H. Chen, and J. Sun, "On physical-layer security in multiuser visible light communication systems with non-orthogonal multiple access," *IEEE Access*, vol. 6, pp. 34004–34017, 2018.
[21] J.-Y. Wang, C. Liu, J.-B. Wang, Y. Wu, M. Lin, and J. Cheng, "Physical-layer security for indoor visible light communications: Secrecy capacity analysis," *IEEE Trans. Commun.*, vol. 66, no. 12, pp. 6423–6436, Jul. 2018, doi: 10.1109/TCOMM.2018.2859943.
[22] A. Mostafa and L. Lampe, "Securing visible light communications via friendly jamming," in *Proc. IEEE Global Commun. Conf. (GLOBECOM), Workshop Opt. Wireless Commun.*, Dec. 2014, pp. 524–529.
[23] H. Zaid, Z. Rezki, A. Chaaban, and M. S. Alouini, "Improved achievable secrecy rate of visible light communication with cooperative jamming," in *Proc. IEEE Global Conf. Signal Inf. Process. (GlobalSIP)*, Dec. 2015, pp. 1165–1169.

[24] H. Shen, Y. Deng, W. Xu, and C. Zhao, "Secrecy-oriented transmitter optimization for visible light communication systems," *IEEE Photon J.*, vol. 8, no. 5, Oct. 2016, Art. no. 7905914.
[25] M. A. Arfaoui, Z. Rezki, A. Ghrayeb, and M. S. Alouini, "On the secrecy capacity of MISO visible light communication channels," in *Proc. IEEE Global Commun. Conf. (GLOBECOM)*, Dec. 2016, pp. 1–7.
[26] T. V. Pham, T. Hayashi, and A. T. Pham, "Artificial-noise-aided precoding design for multi-user visible light communication channels," in *Proc. IEEE Int. Conf. Commun. (ICC), Workshop Opt. Wireless Commun.*, May 2018, pp. 1–6.
[27] J. G. Smith, "The information capacity of amplitude and variance-constrained scalar Gaussian channels," *Inf. Control*, vol. 18, pp. 203–219, Apr. 1971.
[28] T. Komine and M. Nakagawa, "Fundamental analysis for visible-light communication system using LED lights," *IEEE Trans. Consum. Electron.*, vol. 50, no. 1, pp. 100–107, Feb. 2004.
[29] T. Cover and J. Thomas, "*Elements of Information Theory*. Hoboken, NJ, USA: Wiley, 2006.
[30] H. Sifaou, K.-H. Park, A. Kammoun, and M.-S. Alouini, "Optimal linear precoding for indoor visible light communication system," in *Proc. IEEE Int. Conf. Commun. (ICC)*, May 2017, pp. 1–5.
[31] A. L. Yuille and A. Rangarajan, "The concave-convex procedure (CCCP)," *Neural Comput.*, vol. 15, no. 4, pp. 915–936, 2003.
[32] B. K. Sriperumbudur and G. R. Lanckriet, "On the convergence of the concave-convex procedure," in *Proc. Neural Inf. Process. Syst.*, 2009, pp. 1–9.
[33] M. S. Lobo, L. Vandenberghe, S. Boyd, and H. Lebret, "Applications of second-order cone programming," *Linear Algebra Appl.*, vol. 284, nos. 1–3, pp. 193–228, Nov. 1998.
[34] A. Wiesel, Y. C. Eldar, and S. Shamai, "Zero-forcing precoding and generalized inverses," *IEEE Trans. Signal Process.*, vol. 56, no. 9, pp. 4409–4418, Sep. 2008.
[35] S. Boyd and L. Vandenberghe, *Convex Optimization*. Cambridge, U.K.: Cambridge Univ. Press, 2004.
[36] M. Grant and S. Boyd. (Jan. 2015). *CVX: MATLAB Software for Disciplined Convex Programming Version 2.1*. [Online]. Available: http://cvxr.com/cvx/
[37] J. Lofberg, "YALMIP: A toolbox for modeling and optimization in MATLAB," in *Proc. IEEE Int. Symp. Comput. Aided Control Syst. Design*, Sep. 2004, pp. 284–289.

THANH V. PHAM (S'13) received the B.E. and M.E. degrees in computer network systems from The University of Aizu, Japan, in 2014 and 2016, respectively, where he is currently pursuing the Ph.D. degree. His study in Japan was funded by the Japanese Government Scholarship (Monbukagakusho). His research interests include the areas of free-space optics, relay networks, and visible light communications. He is a Student Member of the IEEE and the IEICE.

TAKAFUMI HAYASHI received the B.E., M.E., and Ph.D. degrees in applied physics from The University of Tokyo, Japan, in 1985, 1987, and 1992, respectively. From 1982 to 1994, he was a Researcher Associate with The University of Tokyo. From 1993 to 2005, he was an Associate Professor with The University of Aizu, where he was a Professor, from 2005 to 2016. Since 2016, he has been a Professor with Niigata University. His current research interests include sequence design, signal processing, image analysis, mobile communications, security management, and social informatics. He is a member of ACM, AMS, APS, EURASHIP, IEEE, IET, SIAM, JASI, JSIAM, JSAP, IPSJ, and SIE.

ANH T. PHAM (M'00–SM'11) received the B.E. and M.E. degrees in electronics engineering from the Hanoi University of Technology, Vietnam, in 1997 and 2000, respectively, and the Ph.D. degree in information and mathematical sciences from Saitama University, Japan, in 2005. From 1998 to 2002, he was with NTT Corporation, Vietnam. Since 2005, he has been a Faculty Member with The University of Aizu, where he is currently a Professor and the Head of the Computer Communications Laboratory, Division of Computer Engineering. His research interests include the broad areas of communication theory and networking with a particular emphasis on modeling, design, and performance evaluation of the wired/wireless communication systems and networks. He has authored/co-authored over 160 peer-reviewed papers on these topics. He is a Senior Member of the IEEE. He is also member of IEICE and OSA.